Turbo Coding for a Coherent DS-CDMA System Employing a MMSE Receiver on a Rayleigh Fading Channel *

Kai Tang, Paul H. Siegel and Laurence B. Milstein

March 2, 2000

Abstract

Previous research which analyzed the performance of a convolutionally coded CDMA system with a MMSE receiver for interference suppression showed that lower rate codes are not always the best choice on Rayleigh fading channels. In this paper, we analyze the performance of a turbo-coded CDMA system with the MMSE receiver. Theoretical bounds are derived based on the optimum tap weights of the MMSE receiver and the tangential bounds of turbo codes. Simulation results incorporating the effects of finite interleaving and RLS adaptation are also presented. The results show that with the MMSE receiver, the high rate turbo code is the best choice. They also show that, except for a bit error rate (BER) lower than 10^{-3}, the capacity of the system is not increased by using turbo codes with small block sizes.

*This work was supported by the National Science Foundation, TRW, CoRe project and Center for Wireless Communcations, UCSD.

1 Introduction

The capacity of a DS-CDMA system is primarily limited by multiple access interference (MAI) and multipath fading. Various multiuser receivers for DS-CDMA systems have been considered over the past few years. In [6], the performance of a convolutionally coded CDMA system with a MMSE receiver for interference suppression has been analyzed. The trade-off between the time diversity, achieved by convolutional coding and interleaving, and the interference suppression, achieved by the adaptive MMSE receiver, was studied. Unlike a CDMA system with a conventional matched-filter (MF) receiver, lower rate convolutional codes are not always the best choice on Rayleigh fading channels.

In this paper, we study the performance of a turbo coded DS-CDMA system with the MMSE receiver on Rayleigh fading channels. The trade-off between the bandwidth allocation of turbo coding and spreading is investigated. In addition, the performance of the turbo coded system is compared to that of a convolutionally coded system with comparable hardware complexity.

This paper is organized as follows. The system and channel models are introduced in Section II. Section III gives the system analysis. Finally, results and conclusions are provided in Sections IV and V, respectively.

2 System and Channel Models

The block diagram of the system under analysis is shown in Fig. 1. The turbo encoder consists of two or more recursive systematic convolutional (RSC) encoders, parallelly concatenated by a permutation. The parity bit

streams are punctured, if necessary, and then transmitted together with the systematic bit stream. At the end of each transmission block, only the first encoder is driven back to the all-zero state using the trellis termination scheme of [4], whereas the remaining encoders are not terminated.

It has been shown that turbo codes using pseudo-random permutation outperform turbo codes using block permutation [11]. The permutation adopted in our system is the so-called "S-Random" permutation [4], which prohibits the mapping of a bit-position to another within a distance $\pm S$ of a bit-position already chosen in any of the S previous selections. As a rule of thumb, for a permutation with block size N, $S < \sqrt{N/2}$ is chosen [4].

The encoded bit streams are serially concatenated and passed to a channel interleaver. The purpose of the interleaver is to separate adjacent code bits in time, so that, ideally, each code bit will experience independent fading. The output of the interleaver is then spread by the signature sequence assigned to the given user and mapped to a sequence of QPSK symbol. For an asynchronous DS-CDMA system, the transmitted signal for the k-th user is given by

$$s_k(t) = \mathrm{Re}\{S_k(t)e^{-j\omega_0 t}\} \tag{1}$$

where

$$S_k(t) = \sqrt{2P_k}a_k(t)b_k(t), \tag{2}$$

P_k is the transmitted power, $b_k(t)$ is the transmitted symbol sequence with period T_s, ω_0 is the carrier frequency, and $a_k(t)$ is the spreading sequence given by

$$a_k(t) = \sum_{n=0}^{N_s-1} a_{k,n}h(t - nT_c). \tag{3}$$

In (3), $a_{k,n} \in \{\pm 1\}$ is the n-th chip of the spreading sequence, N_s is the processing gain, $h(t)$ is the impulse response of the chip pulse shaping filter assumed to satisfy the constraint $\int_{-\infty}^{\infty} |H(f)|^2 df = 1$, and $1/T_c$ is the chip rate. Since it is necessary to have the statistics of MAI to be cyclostationary for the MMSE receiver, short spreading sequence are used, so that $T_s = N_s T_c$.

The channel is modeled as a slowly-varying, frequency non-selective Rayleigh fading, along with AWGN. The received signal is given by

$$R(t) = \sum_{k=0}^{K-1} \alpha_k e^{j\psi_k} S_k(t - \tau_k) + N(t) \tag{4}$$

where α_k is a normalized Rayleigh random variable, ψ_k is the random phase uniformly distributed over $[0, 2\pi)$, τ_k is the delay experienced by the k-th user, and $N(t)$ is a low-pass equivalent, complex AWGN with $E[N(t_1)N^*(t_2)] = 2N_0\delta(t_1 - t_2)$. We assume that τ_k is uniformly distributed in the interval $[0, T_s)$, and can be written as $\tau_k = p_k T_c + \delta_k$, where $p_k = 0, 1, \cdots, N_s - 1$ with equal probability, and δ_k is uniform on $[0, T_c)$. Without loss of generality, index $k = 0$ is assigned to the desired user, and we assume $\tau_0 = 0$ and $\psi_0 = 0$ (perfect bit synchronization and carrier recovery).

After down-conversion, the received signal passes through a chip matched-filter with a normalizing factor of $\frac{1}{\sqrt{2P_0}T_c}$, and then a linear, adaptive filter with N_s taps [9]. The output of the adaptive filter is fed into a block interleaver and an iterative turbo decoder which outputs the estimated data.

3 Analysis

3.1 MMSE receiver

Assume we can independently track the phase of the desired user and remove it from the received signal prior to entering the MMSE receiver. In this case, the output of the coherent demodulator and adaptive filter with tap weights $\mathbf{c}^i$ is given by

$$U_i = \mathbf{c}^{iT}\mathbf{R}^i_{MF}e^{-j\psi^i_0} \tag{5}$$

where $\mathbf{R}^i_{MF} = \mathbf{R}^i_0 + \mathbf{R}^i_N + \mathbf{R}^i_{ma}$, and $\mathbf{R}^i_0$, $\mathbf{R}^i_N$ and $\mathbf{R}^i_{ma}$ are N_s element column vectors corresponding to the desired user's signal, the AWGN and the MAI, respectively. It can be shown [6] that $\mathbf{R}^i_0 = \alpha^i_0 e^{j\psi^i_0} b^{(i)}_0 \mathbf{a}_0$ and

$$\mathbf{R}^i_{ma} = \sum_{k=1}^{K-1} \sqrt{\frac{P_k}{P_0}} \alpha^i_k e^{j\psi^i_k} \mathbf{I}^i_k, \tag{6}$$

where

$$\mathbf{I}^i_k = \mathbf{d}^{(p^i_k)}(1 - \frac{\delta^i_k}{T_c}) + \mathbf{d}^{(p^i_k+1)}\frac{\delta^i_k}{T_c}, \tag{7}$$

$\mathbf{d}^{(q)} = [b^{(i-1)}_k a^{(-q)}_k, b^{(i-1)}_k a^{(-q+1)}_k, \cdots, b^i_k a^{(0)}_k, \cdots, b^i_k a^{(N_s-1-q)}_k]^T$, $b^{(j)}_k$ is the k-th user's symbol transmitted during the time interval $[jT_s, (j+1)T_s)$, and $a^{(l)}_k$ is the l-th chip from the k-th user's spreading sequence. The elements in R^i_N are independent, complex Gaussian random variables with zero mean and variance $\sigma^2_N = \frac{N_0}{E_s}N_s$, where $E_s = P_0 T_s$ is the transmitted symbol energy.

The optimum tap weights, found by the solution of the Wiener-Hopf equation which minimizes the mean square error $J(i) = E|U_i - b^i_0|^2$, is given by

$$\mathbf{c}^i_{opt} = R^{-1}_i \mathbf{p}_i \tag{8}$$

where $\mathbf{p}_i \triangleq E[b_0^{(i)}\mathbf{R}_{MF}^{i*}e^{j\psi_0^i}] = B_o^i\mathbf{a}_0$, and

$$R_i \triangleq E[\mathbf{R}_{MF}^i\mathbf{R}_{MF}^{iH}] = A_0^i\mathbf{a}_0\mathbf{a}_0^T + \sigma_N^2\mathrm{I}_{N_s\times N_s} + \sum_{k=1}^{K-1}\frac{P_k}{P_0}A_k^iE[\mathbf{I}_k^i\mathbf{I}_k^{iH}]. \qquad (9)$$

The two possibilities for A_k^i and B_0^i depend upon the adaptive receiver's ability to track the time-variations of the fading channels. If the fading for the k-th user changes relatively fast and cannot be tracked, then $A_k^i = E[(\alpha_k^i)^2]$ and $B_k^i = E[\alpha_k^i]$. If the adaptive algorithm can track the fading on the k-th user, then $A_k^i = (\alpha_k^i)^2$ and $B_k^i = \alpha_k^i$.

The following analysis assumes that the receiver has perfect knowledge of the channel state information (CSI) and the optimal MMSE filter coefficients, and that infinite interleaving results in independent fades on each symbol. As shown in [6], the output of the adaptive filter can be modeled as a conditionally complex Gaussian random variable as the number of interfering users goes to infinity, based upon the Liapounoff version of the Central Limit Theorem [5]. Even for a small number of users, the Gaussian approximation has been shown to yield accurate results [12]. Conditioned on $\{b_0^{(i)}\}$, $\{\alpha_0^i\}$ and $\{\mathbf{c}_{opt}^i\}$, the output of the adaptive filter for the i-th symbol is modeled as a complex Gaussian random variable with mean $\mu_i \triangleq E[U_i] = \alpha_0^i b_0^{(i)}\mathbf{c}_{opt}^{iT}\mathbf{a}_0$ and variance $\sigma_{U_i}^2 \triangleq E|U_i - \mu_i|^2 = (\mathbf{c}_{opt}^{iT}\mathbf{a}_0)^2/\mathbf{a}_0^T\tilde{R}_i^{-1}\mathbf{a}_0$, where

$$\tilde{R}_i = \mathrm{I}_{N_s\times N_s} + \sum_{k=1}^{K-1}\frac{P_k}{P_0}A_k^iE[\mathbf{I}_k^i\mathbf{I}_k^{iH}]. \qquad (10)$$

Conditioning on the optimum tap weights simply refers to conditioning on the delays and fades of all interfering users which are assumed to be tracked by the adaptive receiver.

3.2 Pairwise Error Probability

For analytical purpose, we assume that a maximum-likelihood (ML) decoder is used to decode the turbo codes. In reality, an iterative decoder will be used and for high enough SNR, empirical evidence indicates that the performance of the ML decoder will be approached as the number of decoding iterations increases.

Since interleaving is done at the coded bit level and QPSK modulation is used, the computed metrics are based on the output of the in-phase (I) and quadrature (Q) channels separately. The ML decoder maximizes the metric given by

$$M_j = \sum_{i=1}^{L} Z_{i,j} \tag{11}$$

where L is the block size of code bits, and

$$Z_{i,j} = \begin{cases} \mathrm{Re}\{U_i\}\alpha_0^i d_{0,j}^{(0)} \mathbf{c}_{opt}^{iT} \mathbf{a}_0, & \text{for the } i\text{-th code symbol on the I-channel} \\ \mathrm{Im}\{U_i\}\alpha_0^i d_{0,j}^{(0)} \mathbf{c}_{opt}^{iT} \mathbf{a}_0, & \text{for the } i\text{-th code symbol on the Q-channel} \end{cases} \tag{12}$$

In (11) and (12), the subscript j refers to a particular codeword, and $d_{0,j}^{(0)}$ is the i-th code symbol of codeword j. Using this metric, the pairwise error probability is given by [6]

$$P_2(d) = Pr[M_j > M_n] \triangleq Pr[Y_d < 0], \tag{13}$$

where j corresponds to any codeword which differs from the correct codeword n in exactly d code symbols, and $Y_d \triangleq M_n - M_j = \sum_{i=1}^{d} y(i)$, where

$$y(i) \triangleq \mathrm{Re}[U_i \alpha_0^i \frac{\mathbf{c}_{opt}^{iT} \mathbf{a}_0}{\sigma_{U_i}^2} (b_{0,n}^{(i)} - b_{0,j}^{(i)})^*]. \tag{14}$$

The contribution from an error in the I-channel or Q-channel in (14) is determined by setting $\mathrm{Im}\{b_{0,n}^{(i)}\} = \mathrm{Im}\{b_{0,j}^{(i)}\}$ or $\mathrm{Re}\{b_{0,n}^{(i)}\} = \mathrm{Re}\{b_{0,j}^{(i)}\}$, respectively.

Since infinite interleaving is assumed, the random variables $y(i)$ are independent for different values of i, with conditional mean and variance given by

$$\mu_y(i) = (\alpha_0^i)^2 \mathbf{a}_0^T \tilde{R}_i^{-1} \mathbf{a}_0 \tag{15}$$

and

$$\sigma_y^2(i) = (\alpha_0^i)^2 \mathbf{a}_0^T \tilde{R}_i^{-1} \mathbf{a}_0, \tag{16}$$

respectively.

Thus, the conditional probability of pairwise error reduces to the following:

$$P_2(d|\{\mathbf{c}_{opt}^i\}, \{\alpha_0^i\}) = Q(\sqrt{2\gamma_d}) \tag{17}$$

where

$$\gamma_d = \frac{(\sum_{i=1}^d \mu_y(i))^2}{\sum_{i=1}^d \sigma_y^2(i)} = \sum_{i=1}^d (\alpha_0^i)^2 \mathbf{a}_0^T \tilde{R}_i^{-1} \mathbf{a}_0 \tag{18}$$

and $Q(x) \triangleq \frac{1}{\sqrt{2\pi}} \int_x^\infty e^{-t^2/2} dt$.

We now further assume that the adaptive algorithm is not able to track the fading on any of the interfering users in the system, and the delays experienced by each user remain constant throughout a transmission block. These assumptions result in $\tilde{R}_i^{-1}$ being independent of i, and γ_d reduces to

$$\gamma_d = \mathbf{a}_0^T \tilde{R}^{-1} \mathbf{a}_0 \sum_{i=1}^d (\alpha_0^i)^2 \tag{19}$$

where $\tilde{R} = \tilde{R}_i$ for any i.

The conditional probability of pairwise error is given by

$$P_2(d|\{\tau_k\}) = (\frac{1-\mu}{2})^d \sum_{k=0}^{d-1} \binom{d-1+k}{k} (\frac{1+\mu}{2})^k \tag{20}$$

with

$$\mu = \sqrt{\frac{\gamma_c}{1+\gamma_c}} \tag{21}$$

and

$$\gamma_c = \frac{1}{2}\mathbf{a}_0^T \tilde{R}^{-1}\mathbf{a}_0. \tag{22}$$

Averaging $P_s(d)$ over $\{\tau_k\}$ is done by taking a sample average of the expressions (20)-(22) for various realization of the delays of all interfering users.

For comparison purposes, we also determined the performance of a matched-filter receiver. If we assume that long spread sequences are employed and the MAI can be modeled as a Gaussian random variable by the Central Limit Theorem, the pairwise error probabilities can be obtained from an expression similar to (20) with γ_c replaced by γ_c^{mf}, where

$$\gamma_c^{mf} = \frac{1}{\frac{2N_0}{E_s} + \frac{4}{3N_s}\sum_{k=1}^{K-1}\frac{P_k}{P_0}} \tag{23}$$

3.3 Performance Bounds

The final union bounds on the frame error rate (FER) and bit error rate (BER) are obtained by summing over all pairwise error probabilities [3]

$$P_e \leq \sum_{d=d_f}^{L} t_d P_2(d) \tag{24}$$

$$P_b \leq \sum_{d=d_f}^{L} c_d P_2(d). \tag{25}$$

Here, t_d is the number of codewords with Hamming weight d, and c_d is the total weight of information bits for codewords with Hamming distance d normalized by the number of information bits per block, N. In order to obtain t_d and c_d, a probabilistic permutation called a "uniform interleaver"

was introduced [2], which represents an average of all possible interleaving permutations. The values of t_d and c_d are then evaluated following the approach given by [3].

The bounds obtained above are upper bounds on the performance of the ML decoder using uniformly interleaved turbo codes. Unfortunately, the union bound becomes quite loose at signal-to-noise ratios (SNR) lower than the thresholds corresponding to the channel cut-off rates, where our interest lies. Here we use a tighter bound, known as the tangential bound [7], to improve the accuracy in the low SNR region.

We have extended the tangential bound for an AWGN channel to a Rayleigh fading channel. The bound on the frame (word) error probability is given by

$$\begin{aligned} P_e \quad \leq \quad & \min_{\rho}\{ \sum_{d=d_f}^{L-N+1} t_d E_{\{\eta_1^{(d)},\eta_2^{(d)}\}}[Q(\sqrt{2\gamma_c\eta_2^{(d)}})Q(\sqrt{\frac{2\gamma_c}{\eta_1^{(d)}}}((1-\rho)\eta_2^{(d)}-\rho\eta_1^{(d)}))] + \\ & (\frac{1-\mu_\rho}{2})^n \sum_{j=0}^{n-1} \binom{n-1+j}{j} (\frac{1+\mu_\rho}{2})^j \} \end{aligned} \tag{26}$$

where $\mu_\rho = \sqrt{\frac{\gamma_c\rho^2}{1+\gamma_c\rho^2}}$, ρ is a parameter to be optimized, and $\eta_1^{(d)}$ and $\eta_2^{(d)}$ are two independent, normalized chi-square distributed random variables, with degrees of freedom $2(n-d)$ and $2d$, respectively. The probability density function of the normalized chi-square distribution with $2d$ degree of freedom is given as

$$f_\eta(x) = \frac{x^{d-1}}{(d-1)!}e^{-x}, \ x > 0 \tag{27}$$

By replacing t_d with c_d, the tangential bound on the bit error probability is obtained. It was proved in [7] that the tangential bound is no looser than the union bound, and its value is always smaller than 1. Fig. 2 compares

the tangential bound on the bit error probability with the union bound and simulation results for a turbo coded BPSK system over an ideally interleaved Rayleigh fading channel. The two turbo codes used in our single-user system are defined in the next section. The improvement of the tangential bound over the union bound is more significant for lower rate codes and codes of large block sizes. Moreover, we can see that for $P_b < 10^{-3}$, there is a degradation in the performance of the rate-1/4 codes with the iterative decoder compared to the bound for the ML decoder, because it has more than two component codes. The improved accuracy of the tangential bound enables us to compare different trade-offs within our system using analytical results.

4 Results

We are interested in the coding-spreading trade-off in a turbo-coded CDMA system. A processing gain of $N_s = 63$ for the uncoded system is assumed. For the MMSE receiver system, the spreading sequences are chosen to be Gold sequences of length 31 for the rate-1/2 codes, and Kasami sequences of length 15 for the rate-1/4 codes. Therefore, the total bandwidth expansion caused by coding and spreading remains roughly the same.

We assume a signal-to-noise ratio of $E_b/N_0 = 15dB$ and perfect power control (i.e., $P_k/P_0 = 1$), unless otherwise specified. The analytical results for the MMSE receiver were obtained by averaging the conditional error probabilities over 1000 realizations of random delays of each user.

For the simulation of finite interleaving systems, the multipath Rayleigh fading was generated using Jakes model [8] with a data rate of 9.6 kbps and a maximum Doppler shift of 83Hz, which corresponds to a carrier frequency

of 900 MHz and a vehicle speed of 100 km/h. The number of information bits per block is set to be N=192, corresponding to a tight delay constraint of 20 ms. A block interleaver was used as the channel interleaver, whose dimensions were chosen to be 48×8 and 48×16, for rate-1/2 and rate-1/4 codes, respectively.

Our rate-1/2 turbo code uses two identical rate-1/2 constituent codes, and the two parity sequences are punctured alternately. For the rate-1/4 turbo code, three identical component codes are used and no puncturing is needed. The constituent codes have a memory length of 2 and the same generator polynomials $(1, \frac{1+D^2}{1+D+D^2})$. The Log-MAP algorithm is used in our iterative decoder [1]. To assure convergence, 15 iterations are used for the rate-1/2 code and 30 iterations are used for the rate-1/4 code. It is claimed in [13] that the processing load of a Log-MAP decoder is no more than four times that of a conventional Viterbi decoder for a convolutional code with the same number of states as the constituent code. So 32-state convolutional codes are used in our results to give roughly comparable hardware complexity.

Fig. 3 compares the upper bounds on the bit error probability for the MMSE receiver and the matched-filter receiver with both rate-1/2 and rate-1/4 turbo codes. The results show that the MMSE receiver provides a significant increase in capacity compared to that of the MF system. In addition, although the MF receiver with lower rate codes outperforms that with higher rate codes, the MMSE systems benefit from high rate codes and larger processing gains when the system is heavily loaded. This is because the number of taps of the MMSE receiver is increased as the processing gain increases, and the capability to suppress interference is also improved. Note that the crossing at $K = 25$ of the performance for the MMSE receivers

with the two code rates is caused by the looseness of the tangetial bound for the rate-1/2 code, thus does not represent the real performance.

Fig. 4 compares the performance of the MMSE receivers with code rates of 1/2 and 1/4, with the level of interference varied by changing the power ratio (P_k/P_0) of all the interfering users in the system. Clearly, the rate-1/2 code with the MMSE receiver is more attractive than the rate-1/4 code when the near-far problem is severe.

Fig. 5 compares the performance of turbo-coded CDMA with that of convolutionally coded systems. Since we are using turbo codes with a relatively small block size, the performances remain approximately the same for the two coding schemes at $P_b = 10^{-3}$, the typical target BER for voice communications. However, for a lower BER (e.g., $P_b = 10^{-5}$), the capacitiy of the system is significantly increased by using the turbo codes. This result indicates that turbo coding is more suitable for data communication applications.

Fig. 6 compares the analytical bounds with simulation results. The simulations assume infinite interleaving and optimum tap weights for the MMSE receiver. The simulation results show that our analytical bounds are good indicators of the performance. Note that our theoretical bounds become loose for BER above 10^{-4}. Moreover, the bounds for rate-1/4 code are not as accurate as those for rate-1/2 code, because the performance of iterative decoder for the rate-1/4 code diverges from that of ML decoder, as shown in Fig. 2. Since the Gaussian approximation tends to be optimistic for low BERs [10], the analytical bounds may be lower than the simulation results for the MF receiver.

Simulation results in Fig. 7 show the performance of the MMSE and MF receivers with finite interleaving and RLS adaptation. For our RLS algo-

rithm, $\lambda = 0.995$ is used as the forgetting factor and 300 training symbols are transmitted before decoding user data. The rate-1/2 turbo code with the MMSE receiver is still the best choice. For the MF receiver, the two code rates give approximately the same performance, because the advantage of a large coding gain of the rate-1/4 code is greatly reduced by the effect of finite interleaving.

Finally, Fig. 8 shows the gradual degradation of performance for the rate-1/2 turbo-coded system with the MMSE receiver as various system assumptions are removed. The biggest reduction of capacity results from finite interleaving, which shows that the delay constraint is a fundamental limit for reliable communication over fading channels. The figure also shows that when perfect CSI is available, the RLS algorithm is able to closely approximate the performance of the MMSE receiver with optimum tap weights.

5 Conclusions

The results of this paper show that the combination of a MMSE receiver and turbo coding can provide a substantial performance improvement compared to conventional matched-filter receiver systems in a multipath fading environment. The MMSE receiver significantly increases the capacity of the system, especially when the near-far problem is severe. For a small block size, turbo codes do not bring much improvement unless a low BER is targeted. Simulation results also show that the system capacity is greatly reduced by the effect of finite interleaving. However, further performance improvement could be expected if looser delay constraints allow the use of turbo codes with larger block size.

References

[1] S. Benedetto, D. Divsalar, G. Montorsi, and F. Pollara. Soft-output decoding algorithms in iterative decoding of turbo codes. *The Telecommunications and Data Acquisition Progress Report*, 42(124):63–87, February 1996.

[2] S. Benedetto and G. Montorsi. Unveiling turbo codes: Some results on parallel concatenated coding schemes. *IEEE Transactions on Information Theory*, 42(2):409–428, March 1996.

[3] D. Divsalar, S. Dolinar, F. Pollara, and R. J. McEliece. Transfer function bounds on the performance of turbo codes. *The Telecommunications and Data Acquisition Progress Report*, 42(122):44–55, August 1995.

[4] D. Divsalar and F. Pollara. Turbo codes for PCS applications. In *Proceedings IEEE International Conference on Communications*, pages 54–59, Seattle, WA, June 1995.

[5] J. R. Foerster. *The Performance of Matched-Filter and MMSE Receivers for DS-CDMA Systems in Multipath Fading Channels*. PhD thesis, University of California, San Diego, 1998.

[6] J. R. Foerster and L. B. Milstein. Coding for a coherent DS-CDMA system employing an MMSE receiver in a Rayleigh fading channel. In *Proceedings of IEEE International Symposium on Information Theory*, Cambridge, MA, August 1998.

[7] H. Herzberg and G. Poltyrev. The error probability of m-ary PSK block coded modulation schemes. *IEEE Transactions on Communications*, 44(4):427–433, April 1996.

[8] W. C. Jakes. *Microwave Mobile Communications*. IEEE Press, 1974.

[9] S. Miller. An adaptive direct-sequence code-division multiple-access receiver for multiuser interference rejection. *IEEE Transactions on Communications*, 43(2/3/4):1746–1755, Feb./March/April 1995.

[10] R. K. Morrow, Jr. and J. S. Lehnert. Bit-to-bit error dependence in slotted DS/SSMA packet systems with random signature sequences. *IEEE Transactions on Communications*, 37(10):1052–1061, October 1989.

[11] L. Perez, J. Seghers, and D. J. Costello Jr. A distance spectrum interpretation of turbo codes. *IEEE Transactions on Information Theory*, 42(6):1698–1709, November 1996.

[12] H. V. Poor and S. Verdu. Probability of error in MMSE multiuser detection. *IEEE Transactions on Information Theory*, 43(3):858–871, May 1997.

[13] A. J. Viterbi. An intuitive justification and a simplified implementation of the MAP decoder for convolutional codes. *IEEE Journal on Selected Areas in Communications*, 16(2):260–264, February 1998.

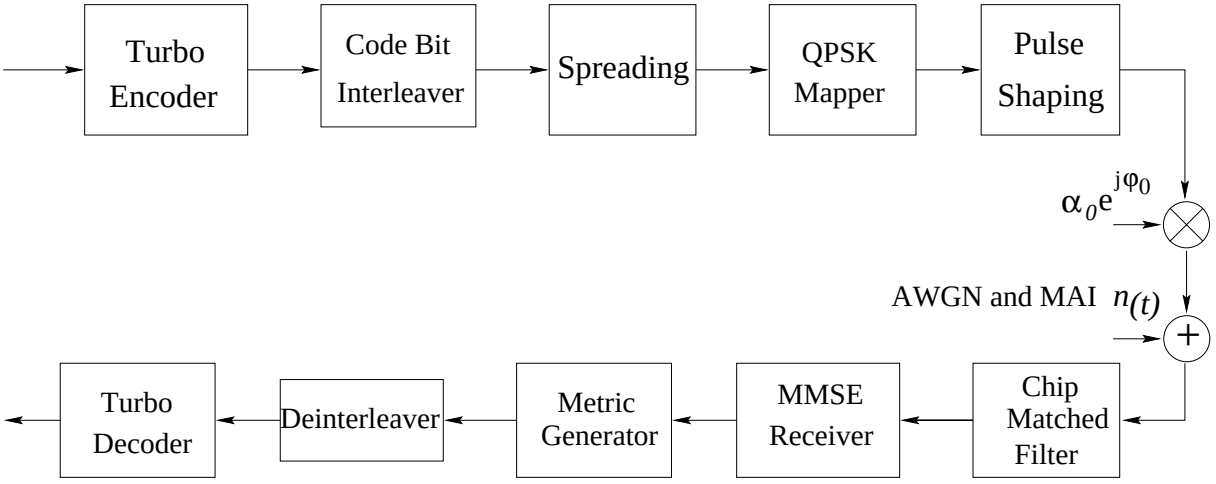

Figure 1: System model

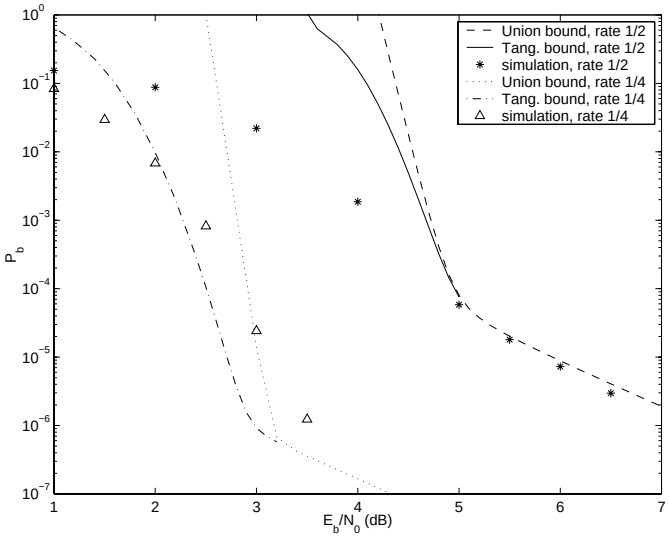

Figure 2: Comparison between tangential bounds and union bounds on bit error probability of turbo codes over Rayleigh fading, assuming infinite interleaving and perfect CSI. The number of information bits per code block is 192.

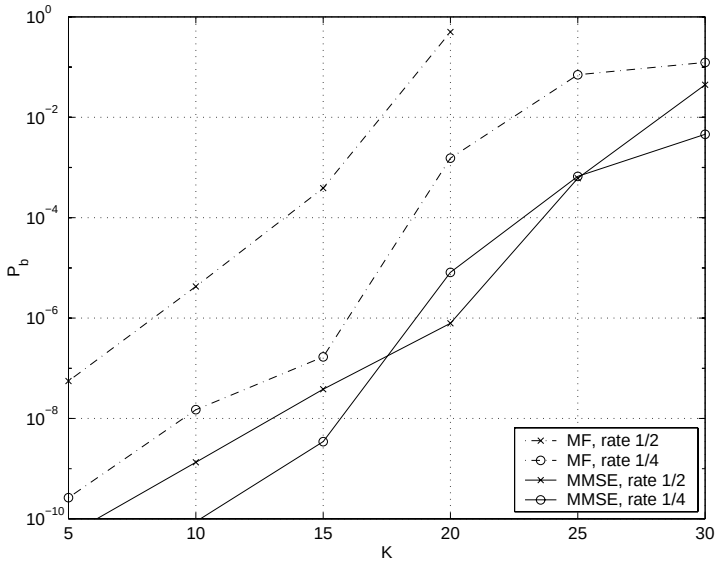

Figure 3: Comparison between matched-filter receiver and MMSE receiver based on theoretical bounds.

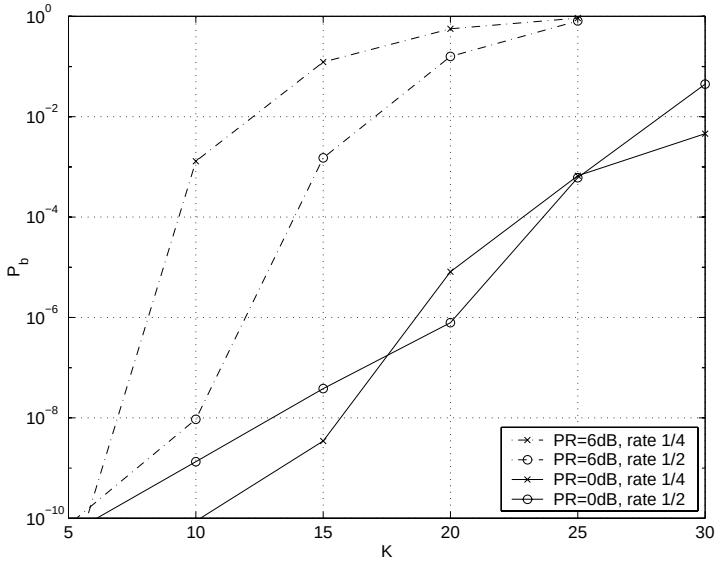

Figure 4: Performance of MMSE receiver with different code rates and power ratios. PR=P_k/P_0 for all interfering users.

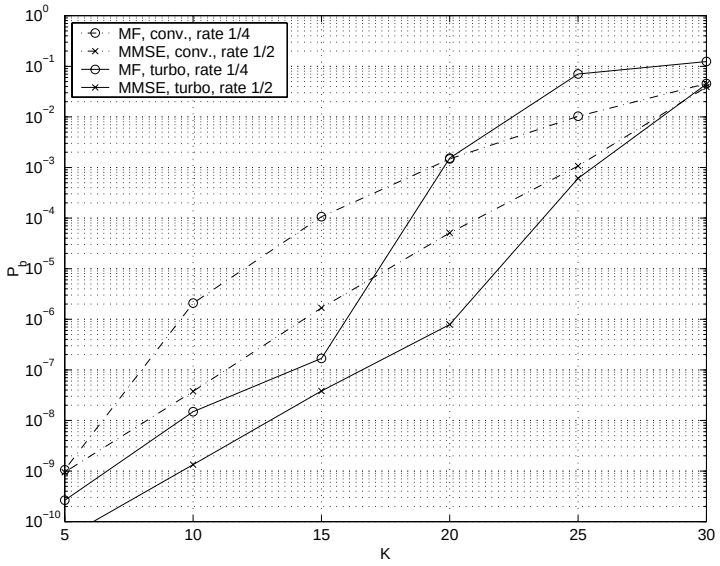

Figure 5: Comparison between convolutionally coded CDMA and turbo-coded CDMA based on theoretical bounds.

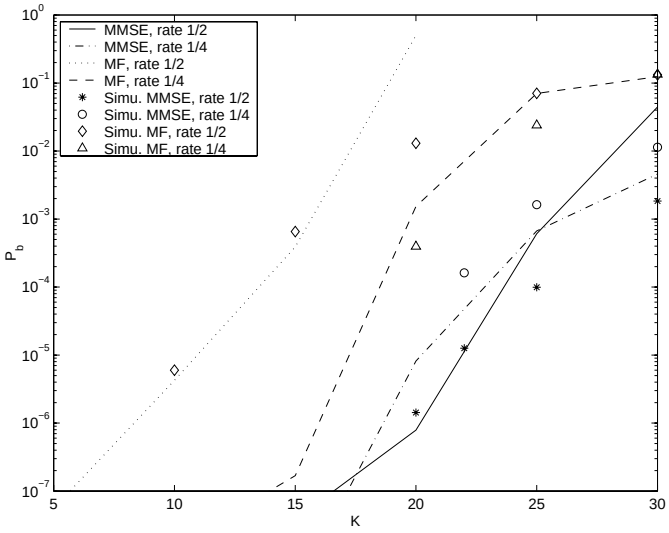

Figure 6: Comparison between analytical bounds and simulation for turbo coded CDMA systems, assuming infinite interleaving and optimum MMSE coefficients.

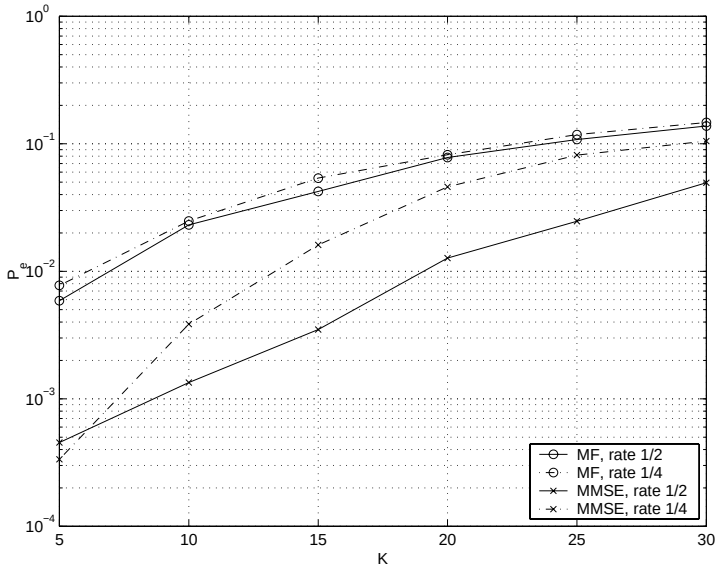

Figure 7: Simulation results for turbo-coded CDMA systems, assuming finite interleaving (20ms delay) and RLS adaptation of MMSE coefficients.

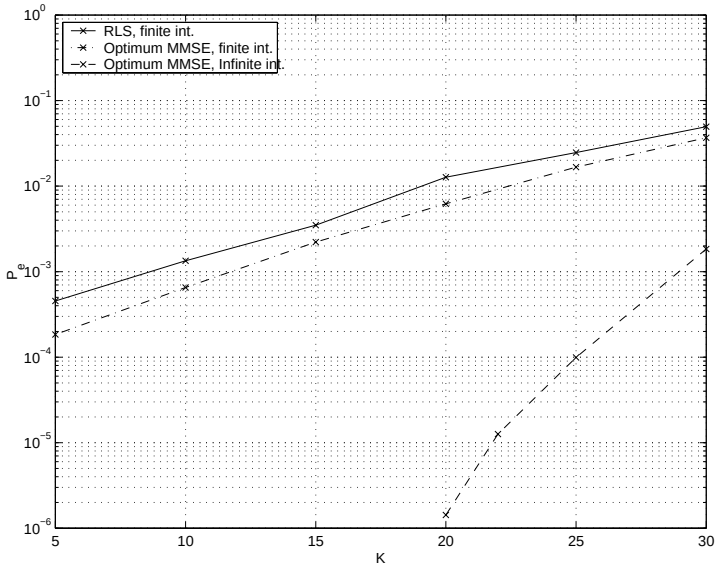

Figure 8: Simulation results for the MMSE receiver with the rate-1/2 turbo code and various system assumptions.